Photoionization with excitation and double photoionization of the Li^+ ground $1\,^1S$ state and metastable $2\,^{1,3}S$ states

U. Kleiman,* M. S. Pindzola, and F. Robicheaux
Department of Physics, 206 Allison Laboratory, Auburn University, Auburn, Alabama 36849-5311, USA
(Received 10 November 2004; revised manuscript received 2 February 2005; published 15 August 2005)

Partial cross-sections for photoionization with excitation of Li^+ leaving the remaining bound electron in the $1s$, $2s$, $2p$, $3s$, $3p$, and $3d$ states and total cross-sections for double photoionization have been calculated employing the time-dependent close-coupling method. The calculations include both the ground state $1s^2\,^1S$ and the two lowest metastable excited states $1s2s\,^{1,3}S$. Photon energies below and up to about 200 eV above the respective thresholds for double ionization are considered. Comparisons are drawn mainly with convergent close-coupling results [A. S. Kheifets and I. Bray, Phys. Rev. A **58**, 4501 (1998)] and *B*-spline based *R*-matrix results [H. W. van der Hart and L. Feng, J. Phys. B **34**, L601 (2001)].

DOI: 10.1103/PhysRevA.72.022707 PACS number(s): 32.80.Fb, 31.15.Ar

I. INTRODUCTION

Photoionization of atoms and ions resulting in the ejection of two or even more electrons cannot occur in the absence of electron-electron correlations due to the single-particle nature of the dipole interaction. This is the reason why double and multiple photoionization processes serve as sensitive probes of electron-electron correlations in both the initial bound and final continuum state. The most basic of all these processes is double photoionization of two-electron systems such as He atoms and Li^+ ions. This process is known as the three-body Coulomb problem and, in full, requires an accurate description of the correlated motion of two electrons in the long-range Coulomb field of the residual stripped atom and ion, respectively. Although this process comprises the interaction of just three charged particles, it can only be handled numerically.

Improvements in computing facilities, synchrotron radiation sources and detection techniques over the last decade have led to highly remarkable advances in the understanding of correlated photoionization processes since the pioneering works [1,2] of the late 1960s. Above all, this applies to the He atom, for which total cross-sections and, more demanding, differential cross-sections for the double photoionization from the ground state $1s^2\,^1S$ have been calculated and measured. Different theoretical methods, like many-body perturbation theory [3,4], the two screened Coulomb method [5–7], the hyperspherical *R*-matrix method with semiclassical outgoing waves [8–10], the convergent close-coupling method [11–15], the *B*-spline based *R*-matrix method [16], the time-dependent close-coupling method [17–21], and, recently, the exterior complex scaling *B*-spline method [22] have been tested. New detection techniques such as the time-of-flight spectroscopy [23–25], the use of toroidal analysers with position-sensitive detectors [26–28], and the cold-target recoil-ion momentum spectroscopy [29–34] have been established. For the two lowest metastable excited states $1s2s\,^{1,3}S$ of He, however, solely theoretical studies of total and differential cross-sections for double photoionization have been performed so far [16,20,35–39]. Unlike the others, the latest investigation [39] is a model calculation which allows one to study the contributions of the two main mechanisms of the double photoionization process, that is, knockout and shake-off.

The situation for double photoionization of ions of the He isoelectronic sequence, which are of importance in plasma physics and astrophysics, is much less advanced, primarily due to difficulties in attaining target densities sufficient to carry out experiments. For Li^+ ions, which, in view of planned comprehensive experiments [40], are the subject of the present paper, to the best of the authors' knowledge, solely calculational results are available to date. Absolute total cross-sections for the ground state $1s^2\,^1S$ of Li^+ ions have been obtained across a wide range of photon energies using uncorrelated and correlated two-electron continuum wave functions, respectively (C2 and C3 models) [41], and the convergent close-coupling method [12]. The former calculation, however, exhibits considerable differences in the cross-sections evaluated in the length and velocity gauges. Calculations for double-to-total and double-to-single cross-section ratios have been made employing the *B*-spline based *R*-matrix method [16] and a model calculation [42] to uncover the two main double photoionization mechanisms as outlined above; the limit of high photon energies has also been considered [43]. Turning to differential cross-sections, till now, there is just one theoretical work dealing with ejected-energy differential cross-sections [41], double and triple differential cross-sections have not been investigated. Presently, less work has been done for the metastable excited states $1s2s\,^{1,3}S$ of Li^+. Double-to-total and double-to-single cross-section ratios for the excited singlet state are available over a fairly wide range of photon energies [16] and in the limit of high photon energies [36] whereas the excited triplet state has been considered for high photon energies [36], only.

Closely related to double photoionization, and likewise impossible in the absence of electron-electron correlations, is photoionization with excitation, that is, just one electron is ejected and the residual ion is left in an excited state. Again, most data are available for the He atom. Apart from many-

*Electronic address: kleiman@physics.auburn.edu

body perturbation theory [44], recent calculations of partial cross-sections for the ground state of He are based on the *R*-matrix with pseudostates method [45], the time-dependent close-coupling method [17], and the convergent close-coupling method [12,15]. Experiments have also been performed, for example, Refs. [46,47]. For the metastable excited states $1s2s\ ^{1,3}S$ of He, data for partial cross-sections are available but solely on the basis of theoretical studies [20,37,38].

Photoionization with excitation of Li^+ has been considered even less. Up to now, it is just the convergent close-coupling method [12] which has been employed for the calculation of absolute partial cross-sections for leaving the remaining bound electron in specified shells, subshells have not been taken into account. This calculation, which covers a wide range of photon energies, has been carried out for the ground state, but not for excited states.

In view of the lack of data for Li^+ ions and planned experiments [40], in this paper the time-dependent close-coupling method, previously applied with great success to the isoelectronic He atom [17–21], is used to look into double photoionization and photoionization with excitation of Li^+ ions, where the ground state and the two lowest metastable excited states $1s2s\ ^{1,3}S$ are considered. The time-dependent close-coupling method is outlined in Sec. II. In Sec. III absolute total cross-sections for double photoionization and absolute partial cross-sections for photoionization with excitation of the remaining bound electron to different subshells are presented and discussed. Comparisons are drawn mainly with convergent close-coupling calculations [12] and *B*-spline based *R*-matrix calculations [16]. Finally, the main results are summarized in Sec. IV.

II. TIME-DEPENDENT CLOSE-COUPLING METHOD

The time-dependent close-coupling method as applied to photoionization with excitation and double photoionization processes in atomic and ionic two-electron systems with an initial $^{1,3}S$ symmetry is outlined below. Atomic units are used unless otherwise stated. A more detailed account, including the implementation of this method on parallel computers, may be found in the initial work [17].

The time-dependent wave function for such atomic or ionic two-electron systems (electron coordinates $\vec{r}_1$ and $\vec{r}_2$) exposed to dipole radiation may be split up into two parts,

$$\Psi_{\text{total}}(\vec{r}_1,\vec{r}_2,t) = \Phi_0^{1,3\text{S}}(\vec{r}_1,\vec{r}_2)e^{-iE_0t} + \Psi^{1,3\text{P}}(\vec{r}_1,\vec{r}_2,t). \quad (1)$$

As shown below, after a sufficient time $t=T_s$ has passed, both absolute partial cross-sections for photoionization with excitation and absolute total cross-sections for double photoionization can be obtained from the time-dependent wave function $\Psi^{1,3\text{P}}(\vec{r}_1,\vec{r}_2,t)$, which initially equals zero.

The wave function $\Phi_0^{1,3\text{S}}(\vec{r}_1,\vec{r}_2)$ for the initial state which, in this paper, is the ground state $1s^2\ ^1S$ or either of the two metastable excited states $1s2s\ ^{1,3}S$ of Li^+, is obtained by an expansion in two-electron coupled spherical harmonics,

$$\Phi_0^{1,3\text{S}}(\vec{r}_1,\vec{r}_2,\tau) = \sum_l \frac{P_{ll}^{1,3\text{S}}(r_1,r_2,\tau)}{r_1 r_2} Y_{ll}^{\text{S}}(\hat{r}_1,\hat{r}_2), \quad (2)$$

and subsequent relaxation of the time-dependent Schrödinger equation

$$-\frac{\partial \Phi_0^{1,3\text{S}}(\vec{r}_1,\vec{r}_2,\tau)}{\partial \tau} = H_{\text{ion}}\Phi_0^{1,3\text{S}}(\vec{r}_1,\vec{r}_2,\tau) \quad (3)$$

in imaginary time ($\tau = it$). The nonrelativistic Hamiltonian operator for the three-body Coulomb system with the nucleus of charge $Z=3$ (Li^+ ions) at the origin of the coordinate system is given by

$$H_{\text{ion}} = -\frac{1}{2}\nabla_1^2 - \frac{Z}{r_1} - \frac{1}{2}\nabla_2^2 - \frac{Z}{r_2} + \frac{1}{|\vec{r}_1 - \vec{r}_2|}. \quad (4)$$

Substituting expansion (2) into Eq. (3) results in a set of coupled partial differential equations for the two-electron radial wave functions $P_{ll}^{1,3\text{S}}(r_1,r_2,\tau)$ which is solved on a numerical lattice consisting of 640×640 points with a mesh spacing of $\Delta r = 0.1$. The solution is obtained by applying low-order finite difference methods as described in Ref. [17]. One starts with

$$P_{ll}^{1\text{S}}(r_1,r_2,0) = P_{1\text{s}}(r_1)P_{1\text{s}}(r_2)\delta_{l,0} \quad (5)$$

for the ground state and with

$$P_{ll}^{1,3\text{S}}(r_1,r_2,0) = \frac{1}{\sqrt{2}}[P_{1\text{s}}(r_1)P_{2\text{s}}(r_2) \pm P_{2\text{s}}(r_1)P_{1\text{s}}(r_2)]\delta_{l,0} \quad (6)$$

for the excited states, where $P_{1\text{s}}(r)$ and $P_{2\text{s}}(r)$ are both bound electron radial wave functions of the Li^{2+} ion. These wave functions and other one-electron radial wave functions $P_{nl}(r)$ used for projection (see below) are calculated by diagonalizing the corresponding time-independent radial Hamiltonian operator,

$$h(r) = -\frac{1}{2}\frac{\partial^2}{\partial r^2} + \frac{l(l+1)}{2r^2} - \frac{Z}{r}, \quad (7)$$

on a one-dimensional numerical lattice having the same number of points and the same mesh spacing as that used for the two-electron system. To set the reader an example, for evaluating a converged fully correlated wave function $\Phi_0^{1\text{S}}(\vec{r}_1,\vec{r}_2)$ and energies for the ground state of Li^+, orbital angular momenta up to $l=8$ were needed in expansion (2) with which Eq. (3) has been time propagated for 750 imaginary time steps of $\Delta\tau = 0.002i$. The comparatively large number of orbital angular momenta is required primarily for photoionization with excitation below the double ionization threshold. For photon energies above the double ionization threshold orbital angular momenta up to $l=5$ are sufficient for most of the calculated cross-sections (see below). The calculational details about the two excited states $1s2s\ ^{1,3}S$ are summarized in Table I. To get converged pure excited-state wave functions, Eq. (3) had to be time propagated over considerable longer imaginary periods. In addition, the relax-

TABLE I. Some details about the generation of the wave function (1) for Li^+ ions in the ground state and in excited states (see text for further explanation).

	$1s^2\ ^1S$	$1s2s\ ^1S$	$1s2s\ ^3S$
Angular momentum l	0,…, (5) 8	0,…, 5	0,…, 5
No. of time steps $\Delta\tau$	750	4000	2750
Time step $\Delta\tau$	$0.002i$	$0.005i$	$0.005i$
Angular momenta l_1, l_2	0,…, (6) 9	0,…, 6	0,…, 6
No. of electric-field periods	25	25	25

ation of the excited singlet state requires a Schmidt orthogonalization, otherwise it would lead to the ground state [48]. Note that for the time-dependent close-coupling method, achieving wave functions which are converged with respect to the number of partial waves, the lattice size, the mesh spacing, and the propagation time is more essential to converging the single and double photoionization cross-sections than generating energies that exactly match the chemical ones.[1] As usual, these parameters were varied until adequate accuracy (about 2–3 %) was achieved. The finite mesh spacing energy results are typically within 1–2 % of the infinite mesh spacing energy results.

The wave function $\Psi_{\text{total}}(\vec{r}_1,\vec{r}_2,t)$ describing the three-body Coulomb system while interacting with a classical time-dependent electric field, satisfies the time-dependent Schrödinger equation which, in the weak-field perturbative limit where one-photon absorption is the only relevant process, reduces to

$$i\frac{\partial \Psi^{1,3\text{P}}(\vec{r}_1,\vec{r}_2,t)}{\partial t} = H_{\text{ion}}\Psi^{1,3\text{P}}(\vec{r}_1,\vec{r}_2,t) + H_{\text{field}}\Phi_0^{1,3\text{S}}(\vec{r}_1,\vec{r}_2)e^{-iE_0t}. \tag{8}$$

Here, the classical electric field of amplitude $E(t)$ and frequency ω is assumed to be fully linearly polarized along the z axis. In the length gauge the corresponding Hamiltonian operator may be written as

$$H_{\text{field}} = E(t)(r_1\cos\theta_1 + r_2\cos\theta_2)\sin(\omega t). \tag{9}$$

To avoid ringing effects, the time-dependent amplitude has to be ramped on quite slowly. Here, it is ramped on linearly from zero to one over a quarter of the total time T_s which is necessary to time propagate Eq. (8) on the already specified numerical lattice for achieving convergence. For both the ground state and the excited states, T_s covers 25 periods of the electric field. Note that one might have also considered a Hamiltonian operator H_{field} in the velocity gauge, but since fully correlated, highly accurate wave functions on the lattice are used for the temporal development of Eq. (8), the results for the partial and total cross-sections, directly extractable from the time evolved wave function $\Psi^{1,3\text{P}}(\vec{r}_1,\vec{r}_2,T_s)$, are expected to be gauge invariant. Previous time-dependent close-coupling calculations of photoionization with excitation and double photoionization of He [17,20] have turned out to be gauge invariant. For the time propagation of Eq. (8), the wave function $\Psi^{1,3\text{P}}(\vec{r}_1,\vec{r}_2,t)$ is expanded in two-electron coupled spherical harmonics

$$\Psi^{1,3\text{P}}(\vec{r}_1,\vec{r}_2,t) = \sum_{l_1,l_2}\frac{P_{l_1l_2}^{1,3\text{P}}(r_1,r_2,t)}{r_1r_2}Y_{l_1l_2}^{\text{P}}(\hat{r}_1,\hat{r}_2) \tag{10}$$

with

$$Y_{l_1l_2}^{\text{P}}(\hat{r}_1,\hat{r}_2) = \sum_{m_1,m_2} C_{m_1m_2M}^{l_1l_21}Y_{l_1m_1}(\hat{r}_1)Y_{l_2m_2}(\hat{r}_2), \tag{11}$$

where $C_{m_1m_2M}^{l_1l_21}$ denotes a Clebsch-Gordan coefficient. In this way, Eq. (8) along with Eq. (9) are transformed into a set of coupled partial differential equations for the two-electron radial wave functions $P_{l_1l_2}^{1,3\text{P}}(r_1,r_2,t)$ to be evaluated, carrying out the time propagation under the initial condition

$$P_{l_1l_2}^{1,3\text{P}}(r_1,r_2,0) = 0 \tag{12}$$

for all possible orbital angular momentum pairs l_1,l_2. For photon absorption from the ground state of Li^+ orbital angular momenta up to $l_1,l_2=9$ have been used to calculate all those cross-sections that will be discussed in Sec. III A. These high orbital angular momenta are mainly necessary for photoionization with excitation processes below the double ionization threshold. For photon energies above the double ionization threshold, orbital angular momenta $l\leqslant 5$ and $l_1,l_2\leqslant 6$ are in general sufficient. Apart from only a few exceptions, the results of the two calculations differ from each other by less than 2%. This, however, does not hold for photoionization with excitation to the subshells $2s$ and $3d$. Here, the inclusion of higher orbital angular momenta has led to a relative decrease of the two partial cross-sections of about 6–9 % and up to 7%, respectively. Moreover, the sum of the partial cross-sections for photoionization with excitation to $2s$ and $2p$ decreases by about 4–6 %. For the two excited states see Table I. Regarding these states it is reasonable to stress that for photon energies below the double ionization threshold an inclusion of higher orbital angular momenta is expected to improve the convergence of some of the partial cross-sections. However, as a sufficient propagation time T_s has to be ensured, the computational resources, available for the present study, do not allow for such more time consuming calculations.

As mentioned briefly, cross-sections for various photoionization processes can be easily extracted from the wave function $\Psi^{1,3\text{P}}(\vec{r}_1,\vec{r}_2,t)$ provided the time propagation according to Eq. (8) has been performed over a period T_s sufficient to ensure convergence. The partial cross-section $\sigma_{nl}^{1,3\text{P}}$ for photoionization with excitation of the remaining bound electron to the subshell nl and the total cross-section $\sigma_{\text{d}}^{1,3\text{P}}$ for double photoionization are given by

[1] In the present calculations, the main source of error in the energy is due to the finite mesh spacing. The electronic correlation, which is a major contributor to double ionization, is accurately represented.

$$\sigma_{nl}^{1,3\mathrm{P}} = \frac{\omega}{I} \left. \frac{\partial \mathcal{P}_{nl}^{1,3\mathrm{P}}}{\partial t} \right|_{t=T_s}, \quad \sigma_{\mathrm{d}}^{1,3\mathrm{P}} = \frac{\omega}{I} \left. \frac{\partial \mathcal{P}_{\mathrm{d}}^{1,3\mathrm{P}}}{\partial t} \right|_{t=T_s}, \quad (13)$$

where $I=10^{15}$ W/cm^2 denotes the intensity of the electric field, that is, the cross-sections are rates divided by the photon flux. Projecting the time evolved wave function $\Psi^{1,3\mathrm{P}}(\vec{r}_1,\vec{r}_2,t)$ onto a complete set of bound electron wave functions for the Li^{2+} ion [see Eqs. (15) and (17) of Ref. [17]] and integrating over the angular coordinates, the probabilities $\mathcal{P}_{nl}^{1,3\mathrm{P}}$ for photoionization with excitation to a bound state nl and $\mathcal{P}_{\mathrm{d}}^{1,3\mathrm{P}}$ for double photoionization may be expressed as follows:

$$\begin{aligned}\mathcal{P}_{nl}^{1,3\mathrm{P}} = & \sum_{l_1} \int_0^\infty dr_1 \left[\int_0^\infty dr_2 P_{l_1 l}^{1,3\mathrm{P}}(r_1,r_2,t) P_{nl}(r_2) \right]^2 \\ & - \sum_{n',l'} \left[\int_0^\infty dr_1 \int_0^\infty dr_2 P_{l'l}^{1,3\mathrm{P}}(r_1,r_2,t) P_{n'l'}(r_1) P_{nl}(r_2) \right]^2 \\ & + \sum_{l_2} \int_0^\infty dr_2 \left[\int_0^\infty dr_1 P_{ll_2}^{1,3\mathrm{P}}(r_1,r_2,t) P_{nl}(r_1) \right]^2 \\ & - \sum_{n',l'} \left[\int_0^\infty dr_1 \int_0^\infty dr_2 P_{ll'}^{1,3\mathrm{P}}(r_1,r_2,t) P_{nl}(r_1) P_{n'l'}(r_2) \right]^2, \end{aligned} \quad (14)$$

$$\begin{aligned}\mathcal{P}_{\mathrm{d}}^{1,3\mathrm{P}} = & \sum_{l_1,l_2} \int_0^\infty dr_1 \int_0^\infty dr_2 P_{l_1 l_2}^{1,3\mathrm{P}}(r_1,r_2,t)^2 - \sum_{n,l} \mathcal{P}_{nl}^{1,3\mathrm{P}} \\ & - \sum_{n,l} \sum_{n',l'} \left[\int_0^\infty dr_1 \int_0^\infty dr_2 P_{l'l}^{1,3\mathrm{P}}(r_1,r_2,t) \right. \\ & \left. \times P_{n'l'}(r_1) P_{nl}(r_2) \right]^2, \end{aligned} \quad (15)$$

where the triangle conditions $\Delta(l_1 l1)$, $\Delta(l'l1)$, $\Delta(l_2 l1)$, and $\Delta(l_1 l_2 1)$ apply. Note that fully evolved in time, the interaction of the electrons becomes quite small in regard to their kinetic energies. Thus projection onto one electron states, here bound electron states, becomes an excellent approximation. Recalling that projections can also be made onto products of distorted continuum electron states yielding the same results for partial and total cross-sections, see, for example, Ref. [20], one may stress that in analogy to real experiments, the projection process corresponds to a pair of free electron detectors. The photoionization probabilities (14) and (15) may be monitored as a function of the propagation time. One can stop time propagating Eq. (8) when the rate of change of the ionization probabilities becomes constant.

III. RESULTS AND DISCUSSION

As mentioned in Sec. II, a major advantage of the time-dependent close-coupling (TDCC) method is the possibility to extract various sorts of cross-sections from the time evolved wave function $\Psi^{1,3\mathrm{P}}(\vec{r}_1,\vec{r}_2,t)$ by applying projection techniques. Here, absolute values for partial and total cross-sections are presented and discussed considering the ground state $1s^2\ ^1S$ and the excited states $1s2s\ ^{1,3}S$ of Li^+ ions.[2] An energy-level diagram showing the relevant levels of Li^+ and Li^{2+} is given for the reader's convenience (see Fig. 1). Comparisons of the TDCC data are made with numerical data of previous calculations wherever possible.

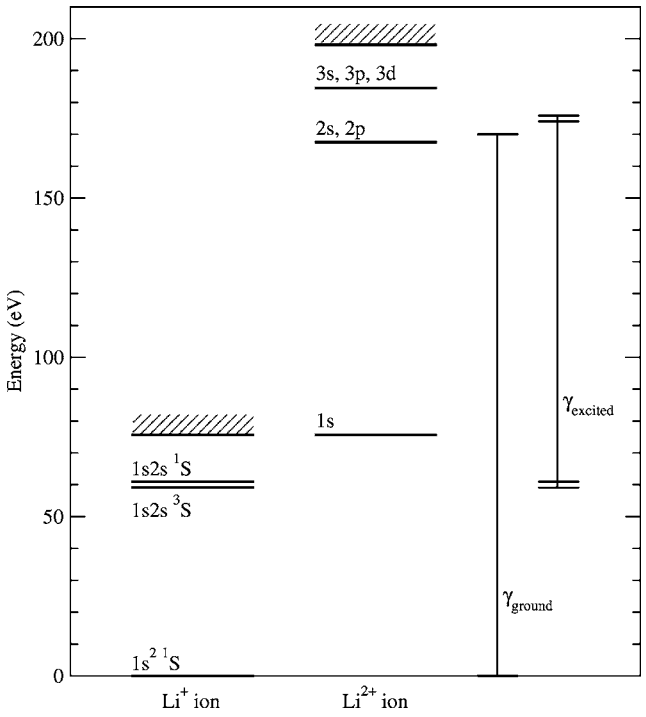

FIG. 1. Energy-level diagram of some of the levels of the Li^+ and Li^{2+} ions. The energies are due to Ref. [49]. γ_{ground} and $\gamma_{excited}$ are the lowest photon energies used to calculate the cross-sections (13) for the ground state $1s^2\ ^1S$ and the two excited states $1s2s\ ^{1,3}S$ of Li^+, respectively.

A. Ground state

Figure 2 displays TDCC partial cross-sections $\sigma_{nl}^{1\mathrm{P}}$ for photoionization with excitation of the ground state of Li^+ ions leaving the remaining bound electron of Li^{2+} in one of the subshells $1s$, $2s$, $2p$, $3s$, $3p$, and $3d$, as well as the summation cross-sections

$$\sigma_2^{1\mathrm{P}} = \sigma_{2\mathrm{s}}^{1\mathrm{P}} + \sigma_{2\mathrm{p}}^{1\mathrm{P}}, \quad \sigma_3^{1\mathrm{P}} = \sigma_{3\mathrm{s}}^{1\mathrm{P}} + \sigma_{3\mathrm{p}}^{1\mathrm{P}} + \sigma_{3\mathrm{d}}^{1\mathrm{P}} \quad (16)$$

for excitation of the remaining bound electron to the shells with principal quantum numbers $n=2$ and $n=3$. Here, photon energies not only above but also below the double ionization threshold (193.5 eV) have been considered. Figure 2 further shows the TDCC total cross-section $\sigma_{\mathrm{d}}^{1\mathrm{P}}$ for double photoionization. Note that the scaling of the four ordinate axes is not uniform as the units Mb$=10^{-18}$ cm^2 and kb$=10^{-21}$ cm^2 are used.

[2]The numerical data are available for making comparisons from the principal author upon request.

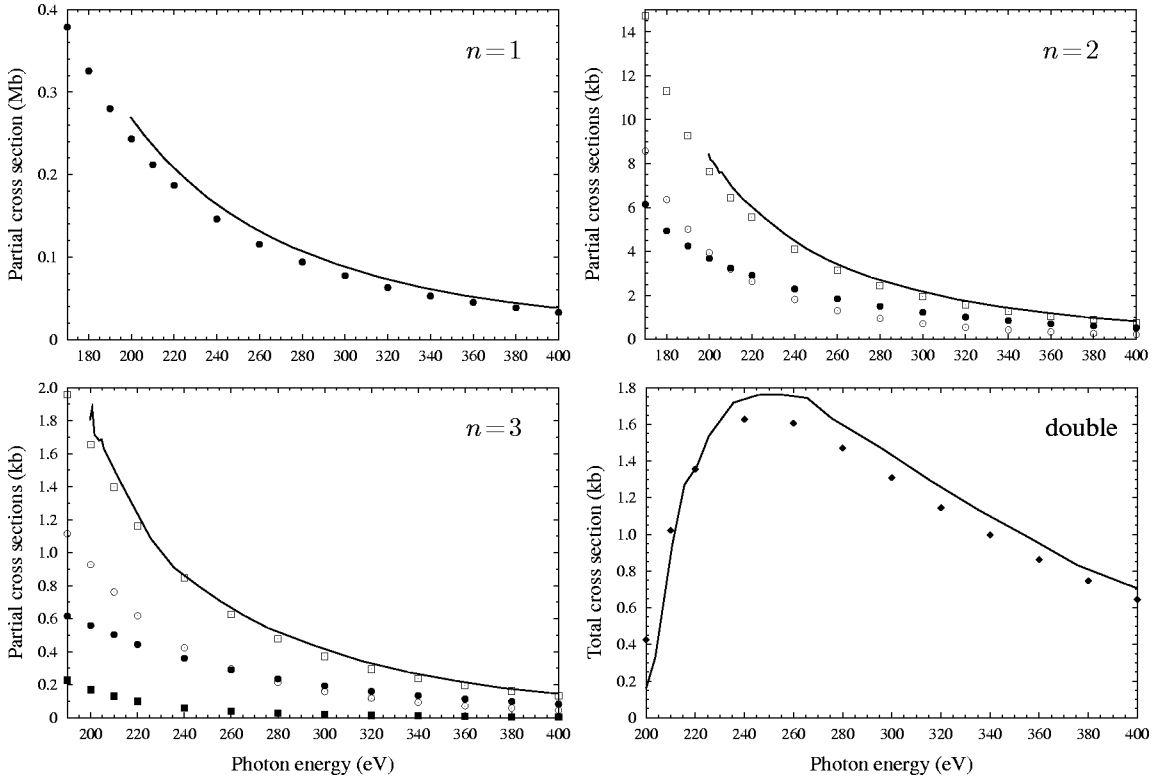

FIG. 2. Partial cross-sections σ_{ns}^{1P} (●), σ_{np}^{1P}(○), σ_{nd}^{1P} (■), and $\sigma_{n}^{1P}=\Sigma_l\sigma_{nl}^{1P}$ (□) for photoionization with excitation and the total cross-section σ_{d}^{1P} (◆) for double photoionization of $Li^+(1s^2, {}^1S)$ ions. The TDCC data are compared to CCC data (——) for the cross-sections $\sigma_{1s}^{1P}, \sigma_{2}^{1P}, \sigma_{3}^{1P}$, and σ_{d}^{1P} [12].

It is obvious from Fig. 2 that photoionization without any excitation is, by far, the dominant process for all photon energies considered because electron-electron correlations are not required. The other processes, for which electron-electron correlations are essential, namely photoionization with excitation and double photoionization, are much less probable. Among the different ionization-excitation processes investigated, excitation of the remaining bound electron to the $n=2$ shell is more likely than to the $n=3$ shell, this particularly applies to the near-threshold region. This finding corresponds with the well-known fact that partial cross-sections become smaller the higher the remaining bound electron is excited as it is more likely that the electron absorbing the photon transfers a small amount of energy to the other electron than a large one. On closer examination, for photon energies below about 210 eV, excitation to the $2p$ subshell is somewhat more likely than to $2s$ indicating a slight preference for the dipole excitation $1s \rightarrow 2p$ compared with the monopole excitation $1s \rightarrow 2s$ at lower photon energies. It is vice versa for higher photon energies. Something similar holds for excitations to the $3s$ and $3p$ subshells where the corresponding partial cross-sections intercept at a photon energy of about 260 eV. The quadrupole excitation from the $1s$ to the $3d$ subshell is the most improbable of all the ionization-excitation processes investigated in this paper. Compared to the latter process, by which one of the two electrons is in a comparatively high excited state, at photon energies of 200 eV and higher double photoionization is more likely to occur. The total cross-section peaks somewhere between 245 and 250 eV and, as anticipated, has the second largest peak of the three total cross-sections for double photoionization (see Figs. 2, 6, and 8) that are examined in this paper.

As mentioned in Sec. I, the number of investigations dealing with photon induced correlated processes in Li^+ ions is comparatively small, and yet, some of the TDCC cross-sections presented in Fig. 2 can be compared with previous calculations, of which the study employing the convergent close-coupling method [12] is the most comprehensive one performed so far. Moreover, this study includes absolute cross-sections.

In the top left part of Fig. 2 the TDCC data for photoionization of $Li^+(1s^2, {}^1S)$ ions with the other electron remaining in the $1s$ shell are compared with the convergent close-coupling (CCC) data evaluated by Kheifets and Bray [12] with the length form of the dipole operator. The overall agreement between the two data sets is good, though for photon energies in the vicinity of the double ionization threshold the CCC data are slightly larger than the TDCC data. This difference becomes smaller for higher photon energies but, within the energy range displayed in the top left part of Fig. 2, the course of the CCC curve is always above the TDCC data points.

The top right and bottom left parts of Fig. 2 display TDCC values of partial cross-sections for photoionization of $Li^+(1s^2, {}^1S)$ ions where the remaining bound electron is excited to the $n=2$ and $n=3$ shells along with the CCC values obtained by Kheifets and Bray [12]. The respective CCC

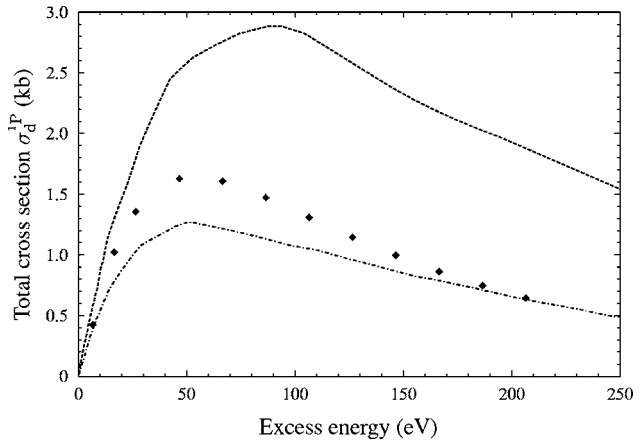

FIG. 3. Total cross-section σ_d^{1P} for double photoionization of $Li^+(1s^2, {}^1S)$ as a function of the energy above the double photoionization threshold: ♦ TDCC data, - - - C2 data (length gauge), -·-·- C2 data (velocity gauge) [41].

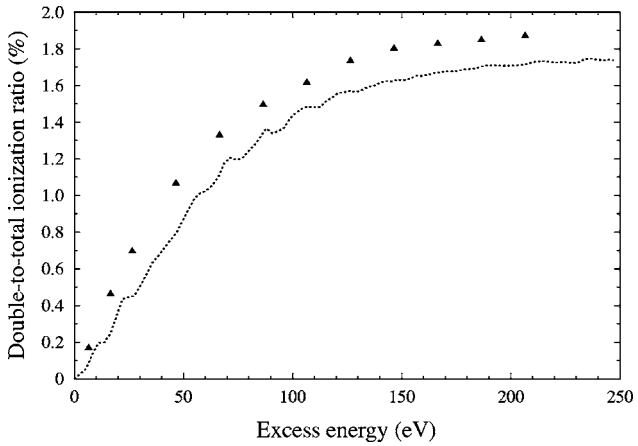

FIG. 4. The ratio between double and total photoionization for $Li^+(1s^2, {}^1S)$ as a function of the energy above the double photoionization threshold: ▲ TDCC data; ···· *B*-spline based *R*-matrix data [16].

curves and TDCC data points almost match each other for photon energies above about 240 eV while for lower photon energies the CCC values are, as for photoionization without excitation, somewhat larger than the TDCC values. The near threshold region for photoionization with excitation to the shells with principal quantum numbers $n=2$ ($\approx$ 167.5 eV [49]) and $n=3$ ($\approx$ 184.5 eV [49]) is particularly sensitive to electron-electron correlations because the electron, which absorbs the incident photon, moves rather slowly and therefore on its way out of the atom has time to interact with the other electron.

For the double photoionization of $Li^+(1s^2, {}^1S)$ ions four calculations employing different theoretical models have been carried out to date [12,16,41,42] where two of them provide absolute total cross-sections so that a direct comparison with the TDCC results is feasible. Beginning again with the CCC calculations of Kheifets and Bray [12], it is evident from the bottom right part of Fig. 2 that there is an overall good agreement between the CCC and TDCC results, though near the double photoionization threshold the CCC value is half the TDCC value. This discrepancy might be due to different double photoionization thresholds calculated by the CCC and TDCC methods where the CCC method seems to yield a threshold value closer to the chemical one [49]. Without exception, for photon energies at and above the peak of the double photoionization cross-section the CCC curve lies slightly above the TDCC data points. As for the prior comparisons experiments would be desirable to perform a more thorough analysis of the CCC and TDCC data, especially as there is just a small difference between these two data sets.

Absolute total cross-sections for the double photoionization of $Li^+(1s^2, {}^1S)$ ions are further available from an older calculation by Kornberg and Miraglia [41] who have used an independent electron approximation (C2 model) in which the double continuum wave function of the final state is built as a product of two Coulomb wave functions. Their results in the length as well as in the velocity form of the dipole operator are sketched in Fig. 3 as a function of the energy above the double photoionization threshold. Though the two reproduced curves are fairly inaccurate as they have been extracted from figures, the huge discrepancy between the length and velocity data is evident. This concerns the magnitude but also the energetic position of the peak of the double photoionization cross-section. The peaks, for example, are separated by about 40 eV. This plainly shows the inability of the C2 model to generate accurate correlated double continuum wave functions for sufficient large ranges. Remember, the length gauge emphasizes the longer range parts of the wave functions whereas the velocity gauge emphasizes the intermediate parts. The TDCC curve, generated with the length form (9) of the dipole operator, falls between the two C2 curves, but it lies vastly much closer to the velocity curve of Ref. [41] and peaks at roughly the same excess energy.

In Fig. 4 the ratio between double and total photoionization obtained by van der Hart and Feng [16], who employed the *B*-spline based *R*-matrix method, is plotted as a function of the energy above the double photoionization threshold. Their data lie systematically below the TDCC data but the shape of the two curves is in good agreement. This may have something to do with the box size as discussed in Ref. [16]. Enlarging the box, which requires additional splines in the basis set and thus more time consuming calculations, most probably results in an increase of the values, especially in the near threshold region. The systematic difference between the two data sets may also be connected with the number of cross-sections that contribute to the total photoionization cross-section. The total photoionization cross-section obtained from the TDCC cross-sections presented in Fig. 2 is as follows:

$$\sigma_{\text{total}}^{1P} = \sigma_1^{1P} + \sigma_2^{1P} + \sigma_3^{1P} + \sigma_d^{1P}. \tag{17}$$

Partial cross-sections for photoionization with excitation of the bound electron to higher shells like $n=4$ and $n=5$ have not been calculated in the present work. The CCC calculations [12], however, indicate that though the partial cross-sections for these excitation processes are considerably

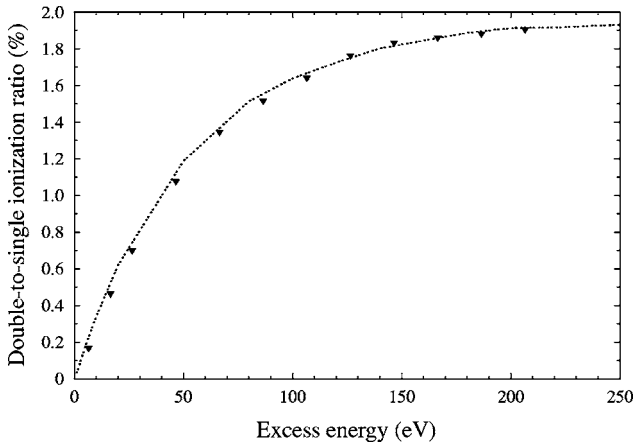

FIG. 5. The ratio between double and single photoionization for $Li^+(1s^2, {}^1S)$ as a function of the energy above the double photoionization threshold: ▼ TDCC data; ·· ·· model calculation data [42].

smaller, they are not necessarily negligible. Therefore the TDCC double-to-total ionization cross-section ratio is expected to decrease and approach towards the *B*-spline based *R*-matrix data. To avoid this problem, in future calculations, the total photoionization cross-section will be directly calculated using the TDCC method.

Another cross-section ratio has been obtained by Schneider and Rost [42], who have made a model calculation as outlined in Sec. I. The double ionization cross-section is normalized to the cross-section for single ionization leaving the residual Li^{2+} ion in its ground state or in an excited state. Their results are displayed in Fig. 5 and are in excellent agreement with the TDCC cross-section ratio which includes ionization with excitation to the shells $n=1$, 2, 3:

$$\sigma_{\text{single}}^{{}^1\text{P}} = \sigma_1^{{}^1\text{P}} + \sigma_2^{{}^1\text{P}} + \sigma_3^{{}^1\text{P}}. \tag{18}$$

Excitations to higher shells, which may result in a slight decrease of the present TDCC values, have not been considered as discussed above.

B. Metastable excited states

Investigating the two metastable excited states $1s2s\ {}^{1,3}S$ of Li^+ ions allows one to probe the influence of the spin symmetry on the two-electron dynamics of photoionization-excitation and double photoionization processes. Although the ionization potentials are lower for the excited states with the two electrons being in different subshells, one might expect the overall electron-electron correlations to be weaker compared to photoionization from the ground state. Unlike the ground state where the incident photon is absorbed by one of the two $1s$ electrons, photon absorption may be through the $1s$ or $2s$ electron of the metastable excited states.

1. Excited singlet state

Figure 6 shows various partial cross-sections $\sigma_{nl}^{{}^1\text{P}}(n \leqslant 3)$ and the summation cross-sections (16) for single photoionization with excitation as well as the total double photoionization cross-section $\sigma_{\text{d}}^{{}^1\text{P}}$ of the metastable excited $1s2s\ {}^1S$

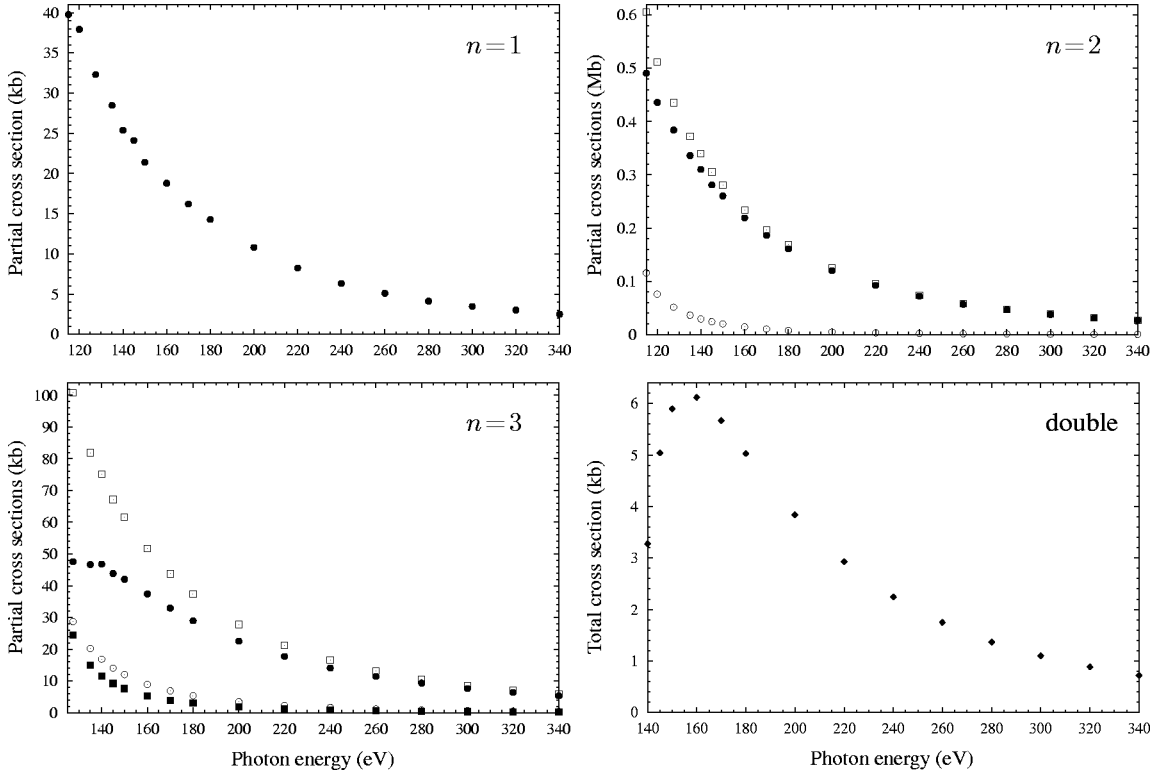

FIG. 6. Partial cross-sections $\sigma_{ns}^{{}^1\text{P}}$ (●), $\sigma_{np}^{{}^1\text{P}}$ (○), $\sigma_{nd}^{{}^1\text{P}}$ (■), and $\sigma_n^{{}^1\text{P}}=\Sigma_l\sigma_{nl}^{{}^1\text{P}}$ (□) for photoionization with excitation and the total cross-section $\sigma_{\text{d}}^{{}^1\text{P}}$ (♦) for double photoionization of $Li^+(1s2s, {}^1S)$ ions.

state of Li^+ ions. As for the ground state, photon energies both above and below the double ionization threshold (134.4 eV) have been considered. Again, note the different scaling of the ordinate axes.

From Fig. 6 it becomes evident that, in contrast to photoionization from the ground state, the residual Li^{2+} ion is much more likely to be left in the $n=2$ and $n=3$ excited states than in the ground state. The corresponding partial cross-sections differ from each other by up to an order of magnitude. As expected, it is by far more probable to find the remaining bound electron in the $n=2$ shell than in $n=3$. This holds for all photon energies investigated. Turning to the subshells, monopole excitation processes are preferred where the remaining bound electron is most likely to be found in the $2s$ subshell. Notice that the latter process does not demand any electron-electron correlations. Therefore photoionization from the excited singlet state is dominated by an uncorrelated process, just as for the ground state. The other uncorrelated process, in which the $2s$ electron of the excited singlet state is ionized, is much less likely to occur. The preferred photoionization of the $1s$ to the $2s$ electron may be understandable in first-order perturbation theory by considering the respective dipole transition matrix elements $M_1 = \langle \varepsilon_1 p\ 2s | D | 1s\ 2s \rangle$ and $M_2 = \langle 1s\ \varepsilon_2 p | D | 1s\ 2s \rangle$. As the total energies of the two final states are the same and the $1s$ electron is more tightly bound than the $2s$ electron, the energy ε_2 is much larger than ε_1. Thus the partial wave $\varepsilon_2 p$ oscillates much more rapidly than $\varepsilon_1 p$, so that M_2 is averaged out much more than M_1. The different shapes of the $1s$ and $2s$ amplitudes seem to be of minor importance. It might be worth mentioning that for photon energies higher than 120 eV, dipole and quadrupole excitation processes yield partial cross-sections which all are of approximately the same order of magnitude. This also holds for the partial cross-section where the bound electron of Li^{2+} is in the ground state. Double photoionization is obviously not the major process but, in comparison to the ground state of Li^+, the total cross-section is significantly larger. It has its peak at about 160 eV photon energy, which is about 25 eV above the double photoionization threshold. Recall that the double photoionization cross-section of the ground state peaks at about 50 eV excess energy where the peak is roughly a factor of three smaller. Anticipating the discussion of the excited triplet state, for double photoionization, the excited singlet state has the largest peak cross-section of all the three initial states investigated here.

As emphasized in Sec. I, up to now only van der Hart and Feng [16] have done calculations on photoionization-excitation and double photoionization of the excited $1s2s\ ^1S$ state of Li^+ ions across a wide range of photon energies. Their double-to-total cross-section ratio is plotted in Fig. 7 versus the excess energy along with the ratio obtained from the TDCC data. As for the ground state, the B-spline based R-matrix values are systematically smaller than the TDCC values. Again, apart from the presence of some nonphysical pseudoresonances [16], the two curves are of similar shape, in particular both curves exhibit a maximum. This is in contrast to the photoionization of the ground state (see Fig. 4) where, for the same excess energies, the double-to-total cross-section ratio continues to increase.

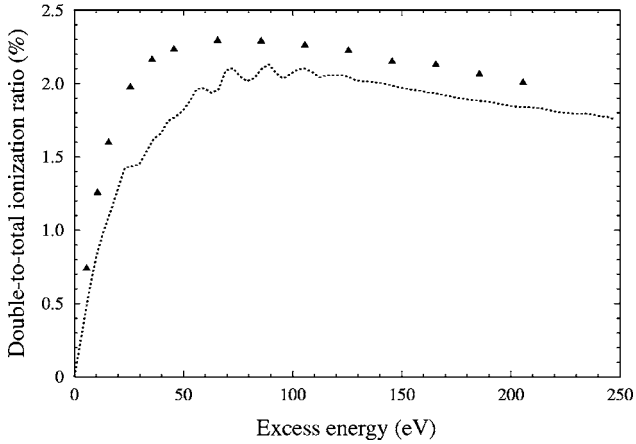

FIG. 7. The ratio between double and total photoionization for $Li^+(1s2s, {}^1S)$ as a function of the energy above the double photoionization threshold: ▲ TDCC data; ···· B-spline based R-matrix data [16].

2. Excited triplet state

The same cross-sections as analyzed for the $1s2s\ ^1S$ state are presented in Fig. 8 for the corresponding excited triplet state. The energy to be expended for double photoionization of this triplet state is slightly smaller as expected; it is 136.3 eV. Again, the four ordinate axes are differently scaled.

Compared to the excited singlet state, it is evident from Figs. 6 and 8 that the parallel orientation of the two electron spins has almost no influence on the magnitude of the partial cross-section for photoionization of Li^+ leaving the residual doubly charged cation in the ground state $1s\ ^1S$. The data point at the incident photon energy of 115 eV might be considered as an exception. A significant increase of 20–30 % relative to the excited singlet state can be made out in the partial cross-section for the photoionization of the excited triplet state where the remaining bound electron is left in the $2s$ subshell. Except for the first data point the partial cross-section where the bound electron is finally in the $2p$ subshell also increases. Though not actually apparent from Figs. 6 and 8, this increase is mainly even larger but, nonetheless, the partial cross-section for $2p$ remains much smaller than the corresponding partial cross-section for $2s$. Thus among the different photoionization-excitation processes investigated, the residual Li^{2+} ion is most likely to be found in the excited $2s$ state. Excitation to any of the subshells of the $n=3$ shell is much less likely. The corresponding summation cross-section, for instance, is about 60–70 % smaller compared to the excited singlet state. Double photoionization is also not the major process among the various correlated processes considered in this paper. For the excited triplet state the total cross-section peaks at a photon energy of about 160 eV. The peak is located at a slightly higher excess energy and is about 90% smaller than the peak of the excited singlet state. Thus this peak is the smallest one. The reason for this is that the excited triplet state has a vanishing probability on the Wannier ridge $r_1 = r_2$ whereas the ground state and the excited singlet state have a nonvanishing probability.

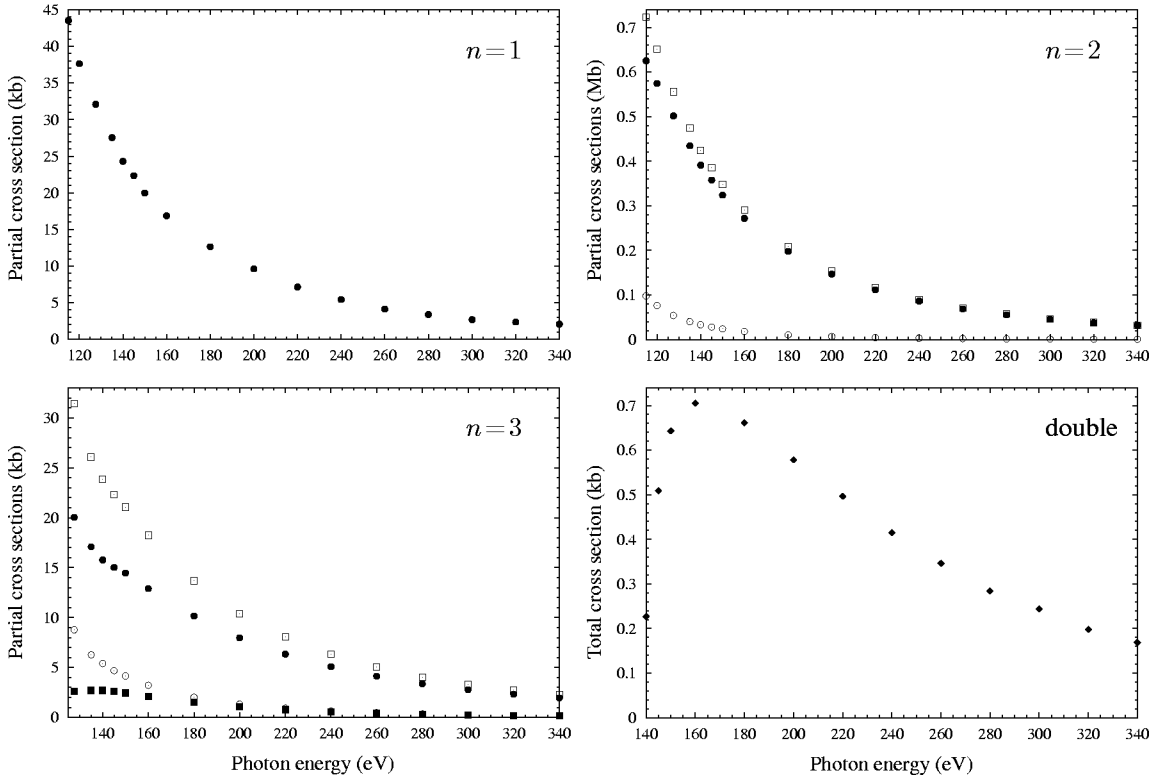

FIG. 8. Partial cross-sections $\sigma_{ns}^{^3\mathrm{P}}$(●), $\sigma_{np}^{^3\mathrm{P}}$(○), $\sigma_{nd}^{^3\mathrm{P}}$ (■), and $\sigma_{n}^{^3\mathrm{P}}=\Sigma_l\sigma_{nl}^{^3\mathrm{P}}$ (□) for photoionization with excitation and the total cross-section $\sigma_{\mathrm{d}}^{^3\mathrm{P}}$ (◆) for double photoionization of $\mathrm{Li}^+(1s2s, {}^3S)$ ions.

Finally, Fig. 9 displays the double-to-single cross-section ratio for photoionization of Li^+ ions being initially in the states $1s^2\ {}^1S, 1s2s\ {}^1S$, and $1s2s\ {}^3S$. It is obvious that double photoionization of the excited singlet state has the largest cross-section ratio. This holds for photon energies up to about 380 eV which is well beyond the threshold for double ionization of the ground state. For photon energies exceeding 380 eV, double ionization of the ground state attains a larger cross-section ratio than double ionization of the excited singlet state. This finding is supported by van der Hart and Feng [16] who considered the ground and excited singlet states and took into account photon energies up to 250 eV above the respective double ionization thresholds. However, it has been shown by Forrey *et al.* [36] that in the limit of high photon energies double ionization of the excited singlet state of Li^+ ions has a larger cross-section ratio than double ionization of the ground state. This means that the respective curves plotted in Fig. 9 must intercept twice. Note that this is in contrast to the He atom [16,36]. As discussed previously, double photoionization of the excited triplet state of Li^+ ions has a considerably smaller cross-section ratio.

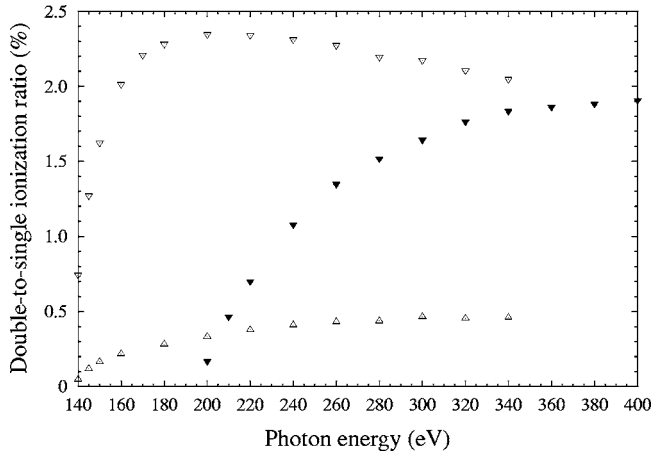

FIG. 9. The ratio between double and single photoionization for the initial states $1s^2\ {}^1S$ (▼), $1s2s\ {}^1S$ (▽), and $1s2s\ {}^3S$ (△) of Li^+ ions.

IV. CONCLUSION

In this paper, an extensive study of photoionization with excitation and double photoionization of the ground state $1s^2\ {}^1S$ and the two metastable excited states $1s2s\ {}^{1,3}S$ of Li^+ ions has been performed employing the time-dependent close-coupling method. The absolute results for the ground state are in good agreement with convergent close-coupling results obtained previously by Kheifets and Bray [12]. They, however, investigated photoionization with excitation to different shells, but not to subshells. Among these processes, the uncorrelated process where the remaining bound electron is left in the $1s$ shell of the Li^{2+} ions dominates. The present time-dependent close-coupling calculation is the very first one providing absolute partial and absolute total cross

sections for the metastable excited states $1s2s\ ^{1,3}S$. The photoionization of both the singlet and the triplet state yields Li^{2+} ions with the bound electron most likely to be found in the $2s$ subshell, a process which does not require electron-electron correlations. For all the three initial states of Li^{+} investigated, double photoionization is much less likely to occur than photoionization with excitation. For photon energies up to about 380 eV, the double-to-single cross-section ratio for photoionization of the excited singlet state is larger than for photoionization of the ground state. From the ratios along with the work of Forrey *et al.* [36] one may conclude that for a limited photon energy region above 380 eV the situation is vice versa. This is in contrast to the He atom [16,36]. The next step in investigating double photoionization of Li^{+} ions is the calculation of differential cross-sections, as they provide more insight into electron-electron correlations.

ACKNOWLEDGMENTS

The authors would like to thank Dr. H. W. van der Hart, Belfast, Dr. A. S. Kheifets, Canberra, and Professor J.-M. Rost, Dresden, for communicating their cross-sections in numerical form and for valuable comments on their calculations. U.K. is further thankful to Dr. J. Colgan, Los Alamos, for initial support in running parallel computer programs. This work was sponsored by the National Science Foundation (NSF) under Grant No. PHY-0098195 with Auburn University. The computational work was carried out mostly at the National Energy Research Scientific Computing Center at Lawrence Berkeley National Laboratory and was further supported by the NSF cooperative agreement ACI-9619020 through computing resources provided by the National Partnership for Advanced Computational Infrastructure at the San Diego Supercomputer Center.

[1] T. A. Carlson, Phys. Rev. **156**, 142 (1967).
[2] F. W. Byron, Jr. and C. J. Joachain, Phys. Rev. **164**, 1 (1967).
[3] K.-I. Hino, T. Ishihara, F. Shimizu, N. Toshima, and J. H. McGuire, Phys. Rev. A **48**, 1271 (1993).
[4] C. Pan and H. P. Kelly, J. Phys. B **28**, 5001 (1995).
[5] D. Proulx and R. Shakeshaft, Phys. Rev. A **48**, R875 (1993).
[6] M. Pont and R. Shakeshaft, J. Phys. B **28**, L571 (1995).
[7] M. Pont, R. Shakeshaft, F. Maulbetsch, and J. S. Briggs, Phys. Rev. A **53**, 3671 (1996).
[8] L. Malegat, P. Selles, and A. Kazansky, Phys. Rev. A **60**, 3667 (1999).
[9] L. Malegat, P. Selles, and A. K. Kazansky, Phys. Rev. Lett. **85**, 4450 (2000).
[10] P. Selles, L. Malegat, and A. K. Kazansky, Phys. Rev. A **65**, 032711 (2002).
[11] A. S. Kheifets and I. Bray, Phys. Rev. A **54**, R995 (1996).
[12] A. S. Kheifets and I. Bray, Phys. Rev. A **58**, 4501 (1998).
[13] A. S. Kheifets and I. Bray, J. Phys. B **31**, L447 (1998).
[14] A. S. Kheifets and I. Bray, Phys. Rev. A **62**, 065402 (2000).
[15] A. S. Kheifets, J. Phys. B **34**, L247 (2001).
[16] H. W. van der Hart and L. Feng, J. Phys. B **34**, L601 (2001).
[17] M. S. Pindzola and F. Robicheaux, Phys. Rev. A **57**, 318 (1998); **58**, 779 (1998).
[18] J. Colgan, M. S. Pindzola, and F. Robicheaux, J. Phys. B **34**, L457 (2001).
[19] J. Colgan and M. S. Pindzola, Phys. Rev. A **65**, 032729 (2002).
[20] J. Colgan and M. S. Pindzola, Phys. Rev. A **67**, 012711 (2003).
[21] J. Colgan and M. S. Pindzola, J. Phys. B **37**, 1153 (2004).
[22] C. W. McCurdy, D. A. Horner, T. N. Rescigno, and F. Martín, Phys. Rev. A **69**, 032707 (2004).
[23] R. Wehlitz, F. Heiser, O. Hemmers, B. Langer, A. Menzel, and U. Becker, Phys. Rev. Lett. **67**, 3764 (1991).
[24] J. C. Levin, G. B. Armen, and I. A. Sellin, Phys. Rev. Lett. **76**, 1220 (1996).
[25] J. A. R. Samson, W. C. Stolte, Z.-X. He, J. N. Cutler, Y. Lu, and R. J. Bartlett, Phys. Rev. A **57**, 1906 (1998).
[26] J. P. Wightman, S. Cvejanović, and T. J. Reddish, J. Phys. B **31**, 1753 (1998).
[27] S. Cvejanović, J. P. Wightman, T. J. Reddish, F. Maulbetsch, M. A. MacDonald, A. S. Kheifets, and I. Bray, J. Phys. B **33**, 265 (2000).
[28] C. Dawson, S. Cvejanović, D. P. Seccombe, T. J. Reddish, F. Maulbetsch, A. Huetz, J. Mazeau, and A. S. Kheifets, J. Phys. B **34**, L525 (2001).
[29] R. Dörner, T. Vogt, V. Mergel, H. Khemliche, S. Kravis, C. L. Cocke, J. Ullrich, M. Unverzagt, L. Spielberger, M. Damrau, O. Jagutzki, I. Ali, B. Weaver, K. Ullmann, C. C. Hsu, M. Jung, E. P. Kanter, B. Sonntag, M. H. Prior, E. Rotenberg, J. Denlinger, T. Warwick, S. T. Manson, and H. Schmidt-Böcking, Phys. Rev. Lett. **76**, 2654 (1996).
[30] R. Dörner, H. Bräuning, J. M. Feagin, V. Mergel, O. Jagutzki, L. Spielberger, T. Vogt, H. Khemliche, M. H. Prior, J. Ullrich, C. L. Cocke, and H. Schmidt-Böcking, Phys. Rev. A **57**, 1074 (1998).
[31] H. Bräuning, R. Dörner, C. L. Cocke, M. H. Prior, B. Krässig, A. S. Kheifets, I. Bray, A. Bräuning-Demian, K. Carnes, S. Dreuil, V. Mergel, P. Richard, J. Ullrich, and H. Schmidt-Böcking, J. Phys. B **31**, 5149 (1998).
[32] M. Achler, V. Mergel, L. Spielberger, R. Dörner, Y. Azuma, and H. Schmidt-Böcking, J. Phys. B **34**, 965 (2001).
[33] A. Knapp, A. Kheifets, I. Bray, Th. Weber, A. L. Landers, S. Schössler, T. Jahnke, J. Nickles, S. Kammer, O. Jagutzki, L. Ph. H. Schmidt, T. Osipov, J. Rösch, M. H. Prior, H. Schmidt-Böcking, C. L. Cocke, and R. Dörner, Phys. Rev. Lett. **89**, 033004 (2002).
[34] A. Knapp, M. Walter, Th. Weber, A. L. Landers, S. Schössler, T. Jahnke, M. Schöffler, J. Nickles, S. Kammer, O. Jagutzki, L. Ph. H. Schmidt, T. Osipov, J. Rösch, M. H. Prior, H. Schmidt-Böcking, C. L. Cocke, J. Feagin, and R. Dörner, J. Phys. B **35**, L521 (2002).
[35] Z. Teng and R. Shakeshaft, Phys. Rev. A **49**, 3597 (1994).
[36] R. C. Forrey, H. R. Sadeghpour, J. D. Baker, J. D. Morgan III, and A. Dalgarno, Phys. Rev. A **51**, 2112 (1995).
[37] H. W. van der Hart, K. W. Meyer, and C. H. Greene, Phys.

Rev. A **57**, 3641 (1998).
[38] A. S. Kheifets, A. Ipatov, M. Arifin, and I. Bray, Phys. Rev. A **62**, 052724 (2000).
[39] A. Emmanouilidou, T. Schneider, and J.-M. Rost, J. Phys. B **36**, 2717 (2003).
[40] A. Landers (private communication).
[41] M. A. Kornberg and J. E. Miraglia, Phys. Rev. A **49**, 5120 (1994).
[42] T. Schneider and J.-M. Rost, Phys. Rev. A **67**, 062704 (2003).
[43] A. Dalgarno and H. R. Sadeghpour, Phys. Rev. A **46**, R3591 (1992).
[44] S. Salomonson, S. L. Carter, and H. P. Kelly, Phys. Rev. A **39**, 5111 (1989).
[45] T. W. Gorczyca and N. R. Badnell, J. Phys. B **30**, 3897 (1997).
[46] J. M. Bizau and F. J. Wuilleumier, J. Electron Spectrosc. Relat. Phenom. **71**, 205 (1995).
[47] R. Wehlitz, I. A. Sellin, O. Hemmers, S. B. Whitfield, P. Glans, H. Wang, D. W. Lindle, B. Langer, N. Berrah, J. Viefhaus, and U. Becker, J. Phys. B **30**, L51 (1997).
[48] I. I. Sobelman, *Atomic Spectra and Radiative Transitions* (Springer, Berlin, 1992).
[49] *NIST Atomic Spectra Database*, http://www.physics.nist.gov/cgi-bin/AtData/main_asd